

## Site-Directed Perturbation of Protein Kinase C-Integrin Interaction Blocks Carcinoma Cell Chemotaxis

Maddy Parsons,<sup>1</sup> Melanie D. Keppler,<sup>1</sup> Adam Kline,<sup>2</sup> Anthea Messent,<sup>2</sup> Martin J. Humphries,<sup>2</sup> Ruth Gilchrist,<sup>1</sup> Ian R. Hart,<sup>1</sup> Corinne Quittau-Prevostel,<sup>3†</sup> William E. Hughes,<sup>3‡</sup> Peter J. Parker,<sup>3</sup> and Tony Ng<sup>1\*</sup>

*Richard Dumbleby/Cancer Research UK Department of Cancer Research, GKT School of Medicine, St. Thomas' Hospital, London SE1 7EH,<sup>1</sup> Wellcome Trust Centre for Cell-Matrix Research, School of Biological Sciences, University of Manchester, Manchester M13 9PT,<sup>2</sup> and Protein Phosphorylation Laboratory, Cancer Research UK London Research Institute, London WC2A 3PX,<sup>3</sup> United Kingdom*

Received 27 February 2002/Returned for modification 4 April 2002/Accepted 22 May 2002

**Polarized cell movement is an essential requisite for cancer metastasis; thus, interference with the tumor cell motility machinery would significantly modify its metastatic behavior. Protein kinase C $\alpha$  (PKC $\alpha$ ) has been implicated in the promotion of a migratory cell phenotype. We report that the phorbol ester-induced cell polarization and directional motility in breast carcinoma cells is determined by a 12-amino-acid motif (amino acids 313 to 325) within the PKC $\alpha$  V3 hinge domain. This motif is also required for a direct association between PKC $\alpha$  and  $\beta$ 1 integrin. Efficient binding of  $\beta$ 1 integrin to PKC $\alpha$  requires the presence of both NPXY motifs (Cyto-2 and Cyto-3) in the integrin distal cytoplasmic domains. A cell-permeant inhibitor based on the PKC-binding sequence of  $\beta$ 1 integrin was shown to block both PKC $\alpha$ -driven and epidermal growth factor (EGF)-induced chemotaxis. When introduced as a minigene by retroviral transduction into human breast carcinoma cells, this inhibitor caused a striking reduction in chemotaxis towards an EGF gradient. Taken together, these findings identify a direct link between PKC $\alpha$  and  $\beta$ 1 integrin that is critical for directed tumor cell migration. Importantly, our findings outline a new concept as to how carcinoma cell chemotaxis is enhanced and provide a conceptual basis for interfering with tumor cell dissemination.**

An early critical step within the metastatic cascade involves cell polarization and directed cell movement. The mechanisms controlling these events, however, are poorly understood. Cell polarization signals can be triggered by the binding of cells to extracellular matrix (ECM) proteins, cytokines or chemoattractants, or ligands that are expressed on the surface of target tissues or vessels. Sensing of these extracellular signals results in a redistribution and trafficking of membrane receptors (1, 19) and/or intracellular signaling proteins, as well as the localized formation of protein complexes which can be stable or transient.

Members of the integrin receptor family are vital in mediating cell matrix adhesion and have been implicated in providing the persistence and directionality for cell motility, as in wound healing (7). Specifically, a number of studies have demonstrated that the  $\beta$ -subunit cytoplasmic domains are involved in the control of cell migration. Thus, the tyrosine residues of the two NPXY motifs in  $\beta$ 1 are important for directed cell migration through integrin substrate-coated filters in response to growth factor chemotactic gradients (22, 23). In fact, when expressed as chimeric receptors connected to heterologous

extracellular domains, such as the interleukin-2 receptor (IL-2R)  $\alpha$  subunit, the  $\beta$ 1 integrin cytoplasmic tail acts as a dominant negative inhibitor of endogenous integrin function (4). Moreover, inhibition of integrin-ECM interactions by GRGDS peptides or inhibitory antibodies was also shown to abolish the persistence or directionality of neural crest cell movement (7).

Protein kinase C (PKC) may be seen as part of the molecular machinery that deciphers temporal and spatial changes in intracellular Ca<sup>2+</sup> and diacylglycerol signals (18). The generation of both second messengers is responsive to changes in the ECM environment perceived by cell surface receptors. Blockade of PKC with calphostin C was shown to inhibit the migration of tumor cells towards a variety of ECM proteins (21).  $\alpha$ v $\beta$ 5-dependent migration of carcinoma cells on vitronectin also requires PKC activation (32). We previously reported that MCF-7 breast carcinoma cells transiently expressing PKC $\alpha$ -GFP (green fluorescent protein) exhibited a significant increase in haptotactic migration towards  $\beta$ 1 substrates (16). Together, these data suggest that the PKC family members play a key role in mediating integrin-dependent tumor cell migration.

Recently, we showed that PKC $\alpha$  associates with the common  $\beta$ 1 integrin subunit and that overexpression of this PKC isoform caused a surface upregulation of this receptor, an effect which was attributable to the PKC $\alpha$  regulatory domain (RD) rather than the kinase domain (16). Upon phorbol ester activation, the integrin was internalized into recycling endosomes in a calcium/phosphoinositide 3-kinase/dynamin-1-dependent

\* Corresponding author. Mailing address: Cancer Research UK London Research Institute, Lincoln's Inn Fields Laboratories, 44 Lincoln's Inn Fields, London WC2A 3PX, United Kingdom. Phone: 44(0) 207-269-3054. E-mail: T.Ng@cancer.org.uk.

† Present address: INSERM U469, 34090 Montpellier, France.

‡ Present address: The Garvan Institute of Medical Research, Sydney, New South Wales 2101, Australia.

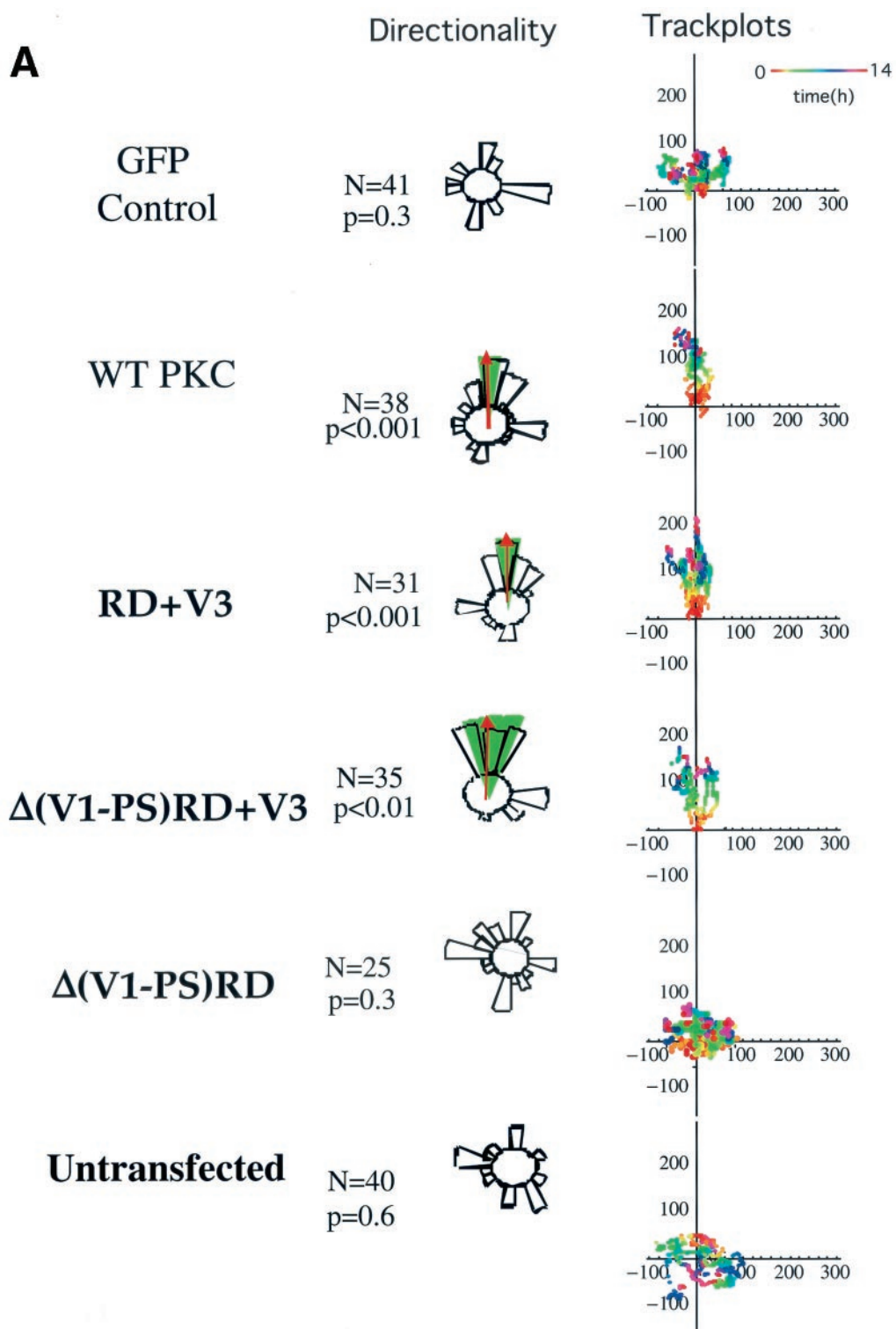


FIG. 1

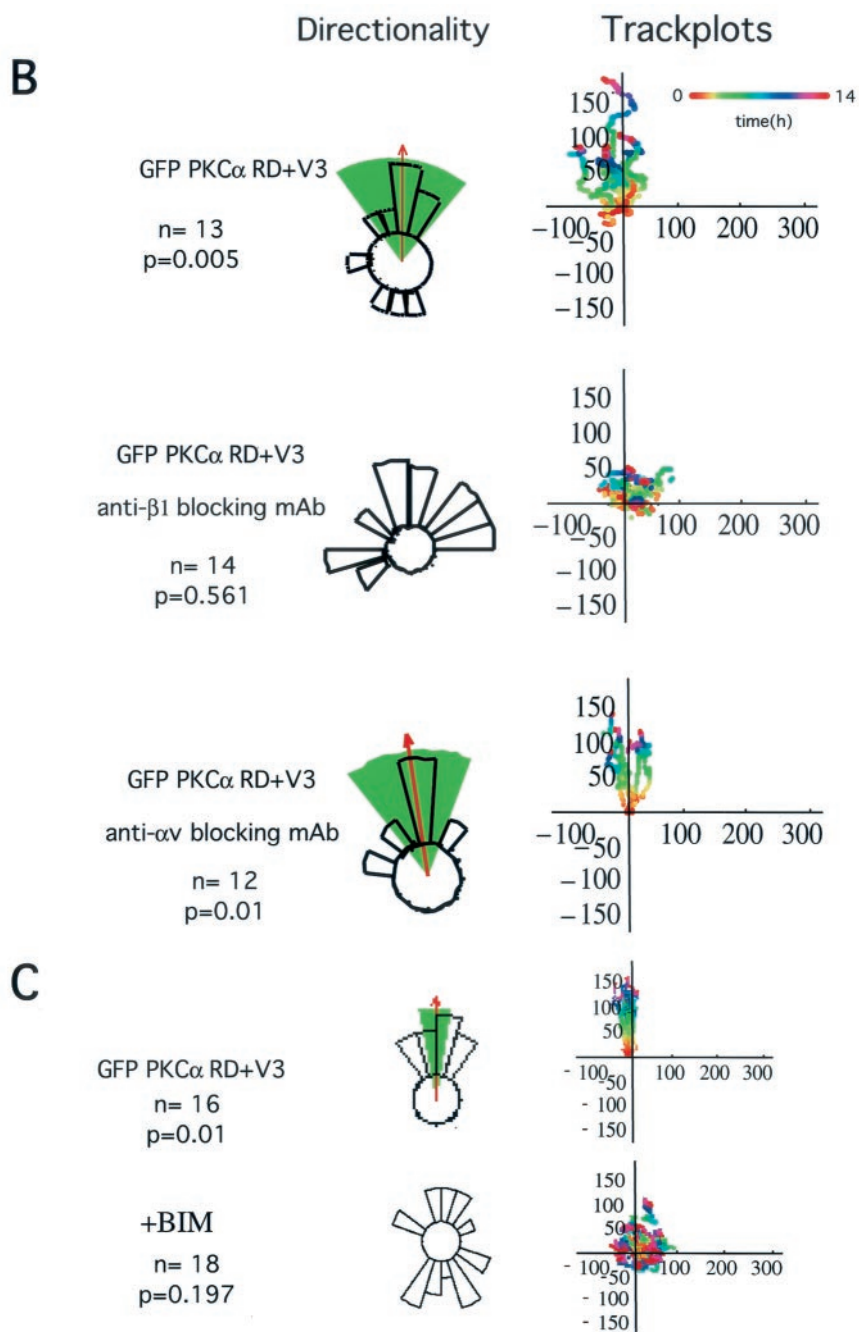


FIG. 1. Effects of different GFP-PKC $\alpha$  RD constructs on MCF-7 cell migration in response to a PDBu gradient. (A) MCF-7 cells expressing full-length GFP-PKC $\alpha$  or two RD constructs with the variable region V3 [GFP-PKC $\alpha$  RD+V3 and GFP-PKC $\alpha$   $\Delta$ (V1-PS)RD+V3] exhibited significant directional chemotaxis towards a PDBu gradient (1  $\mu$ M in the outer well of the Dunn chamber) ( $P < 0.001$ ,  $P < 0.001$ , and  $P < 0.01$ , respectively). Cells transiently expressing the GFP-PKC $\alpha$ (V1-PS)RD construct, which does not contain the V3 region, or the empty vector, displayed no directionality towards the gradient ( $P = 0.3$ ). Untransfected cells exhibited no significant directional motility. Analysis of tracked cells from three independent experiments in comparison to vector-alone equivalents was performed using ANOVA. Significant directional chemotaxis towards the PDBu gradient ( $0^\circ$ ) is represented by a highlighted arc, and the corresponding  $P$  value is shown where relevant. The total number of cells tracked ( $N$ ) is shown. The track plots show all the cell trajectories during the entire time course of each experiment. Each dot represents a cell position at a particular time point which is indicated by the pseudocolor scale (time in hours) beneath each set of cell tracks. The cell track axes are in micrometers. (B) Directional cell motility of cells expressing GFP-PKC $\alpha$  RD+V3 was dependent on  $\beta$ 1, but not  $\alpha$ V, integrin function. Transiently transfected cells were either left alone or preincubated for 1 h with an anti- $\beta$ 1 (P4C10) or anti- $\alpha$ V integrin (L230) inhibitory MAb (10  $\mu$ g/ml), before subjected to the chemotaxis assay described above for panel a, in the presence of the corresponding blocking antibody. (C) Directional cell movement of cells expressing GFP-PKC $\alpha$  RD+V3 was inhibited by bisindolylmaleimide (BIM).

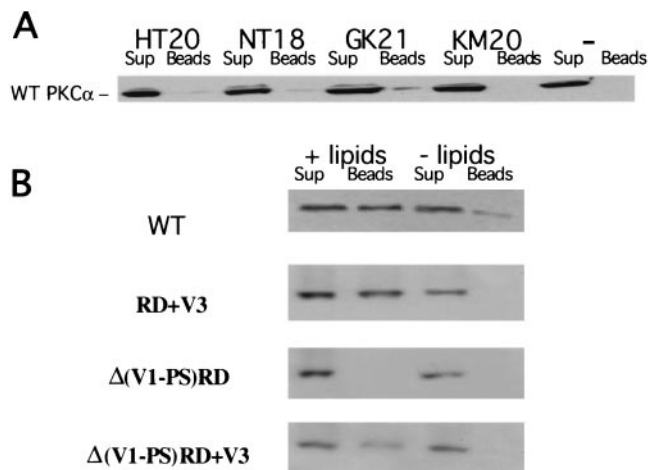


FIG. 2. The third variable domain (V3) is required for the lipid-dependent binding of PKC $\alpha$  to a  $\beta$ 1 integrin cytoplasmic peptide containing both Cyto-2 and Cyto-3 amino acid motifs. Four N-terminally biotinylated, overlapping peptides based on the cytoplasmic sequence of human  $\beta$ 1 integrin were synthesized: KM (aa757-776), KLLMIHHRREFAKFEKEKM; HT (aa763-782), HDRREFAKFEKEKMNKAWDT; NT, (aa777-794), NAKWDTGENPIYKSAVTT; GK, (aa783-803), GENPIYKSAVTTVVNPKYEGK. (A) In an *in vitro* pull-down assay (described in Materials and Methods), full-length GFP-PKC $\alpha$  was most efficiently bound to the  $\beta$ 1 integrin Cyto-2- and Cyto-3-containing peptide GK. For each sample, all of the peptide-bound GFP-PKC $\alpha$  (Beads) was run alongside one-fifth of the corresponding supernatant containing unbound proteins (Sup). The negative-control lane (-) indicates incubation with streptavidin-coupled agarose beads alone. Immunodetection was performed using an anti-GFP polyclonal antiserum (Clontech). The figure shows a representative result of three experiments. (B) The lipid or activator requirement for WT PKC $\alpha$  and different GFP-tagged PKC $\alpha$  RD constructs to bind to the  $\beta$ 1 integrin Cyto domain peptide GK21 *in vitro* was investigated by preincubating the cell extracts containing the different PKC $\alpha$  constructs with mixed micelles containing PS and TPA (+ lipids), compared with no-lipid or no-activator control (- lipids).

manner. The present study reports the mapping of the  $\beta$ 1 cytoplasmic tail binding site on PKC $\alpha$  to a 12-amino-acid region within the V3 hinge sequence of the RD. Furthermore, we show that this hinge domain sequence binds specifically to the distal region (containing the Cyto-2 and Cyto-3 domains) of the  $\beta$ 1 cytoplasmic tail. When incorporated as a minigene insert within a retroviral vector used to infect human breast carcinoma cells, this integrin cytoplasmic domain sequence caused a striking reduction in PKC- and epidermal growth factor (EGF)-driven chemotaxis.

#### MATERIALS AND METHODS

**Cell culture and transfection.** The human breast carcinoma cells (MCF-7 and MDA-MB-231) and the Phoenix amphotropic retroviral packaging cells (Stanford University, Palo Alto, Calif.) were all cultured in Dulbecco's modified Eagle's medium containing 10% fetal calf serum at 37°C. MCF-7 cultures were grown in media supplemented with insulin (10  $\mu$ g/ml). Typical efficiencies of transfection with Lipofectamine Plus (Gibco) were 40% (for various GFP-PKC $\alpha$  constructs), 35% (for IL-2R- $\beta$ 1A integrin chimeras), and 15% (for pECE- $\beta$ 1A).

**Plasmid constructs.** The construction of the GFP-PKC $\alpha$  plasmid and various GFP-RD constructs of PKC $\alpha$  has been described elsewhere (15-17, 27). These RD constructs were subcloned into a vector (dsRed; Clontech) tagged with red fluorescent protein (RFP), using the *EcoRI* and *KpnI* restriction sites.

The GFP-C2V3 construct was generated using primers 5'-GGGGAATTCGATGCACACTGAGAAGAGGGGGCGGATTACC and 3'-GGGGTCGAC

GGCGTGAGTTTCACTCGGTCGAAGG. PCR products were then cloned into the GFP-N1 vector (Clontech) using the *EcoRI* and *SaI* restriction sites. The wild-type (WT) GFP-PKC $\alpha$  plasmid was used as a template to generate the GFP-PKC $\alpha$  V3 truncation constructs. The same 5' primer 5'-GGGGAATTCATGGCTGACGTTTTCCCGGGC-3' was used in all PCRs, and the 3' primers were aa1-337 (amino acids 1 to 337) (5'-GGGGTCGACGGCGTGAGTTTCACTCGGTCGAAGG-3'), aa1-325 (5'-GGGGTCGACGGTTTCTGTCTTTCAGAGGGACTG-3'), 1-313 (5'-GGGGTCGACGGAGCAGGGCCAAAGTTTGGCTTTC-3'), and aa1-301 (5'-GGGGTCGACGGGAGTTCATGTTTCTTCTCC TCG-3'). PCR products were then ligated back into the pCMVIL2R (RC)-INTRA vector using the *HindIII* and *XhoI* restriction sites. Retroviral vectors encoding  $\beta$ 1 cytoplasmic tail peptide and equivalent scrambled peptides were made by generating full-length sense and antisense oligonucleotides (GK21 sense [GGGGAATTCATGGGTGAAAATCTATTATAAGAGTGCCGTAACAACGTGGTCAATCCGAAGTATGAGGGAAAAGAGCAGAAGCTGATCTCAGAGGAGGACCTGTAGGTGACGGG] and GK21 antisense [CCCGTCGACCTACAGGTCCTCTCTGATGATCAGCTTCTGCTCTTTTCCTCATACTTCGGATTGACCAAGTTGTTACGGCAGCCTTATAAATA GGATTTTACCCATGAATTCCCC]) encoding the entire peptides, including a myc tag, and flanked with *EcoRI* and *SaI* restriction sites. Equal volumes of sense and antisense oligonucleotides were heated to 90°C in buffer, allowed to cool slowly, digested with the relevant restriction enzymes, and ligated into the pBABE<sup>pro</sup> retroviral backbone.

**Antibodies and direct conjugation to fluorophores.** MC5 is a murine monoclonal antibody (MAb) that recognizes the V3 region of PKC $\alpha$  (33). P4C10, an anti- $\beta$ 1 blocking antibody, was obtained from Chemicon. Anti- $\alpha_v$  blocking antibody (L230) was obtained from American Type Culture Collection (Rockville, Md.). A MAb against glutathione S-transferase (GST) was used for Western blotting (Zymed Laboratories). Fab fragments were generated and isolated from mouse immunoglobulin G (IgG) using the ImmunoPure Fab preparation kit (Pierce) according to the manufacturer's protocol. Direct conjugation of IgG or IgG Fab fragments to the fluorophore Cy3 (Amersham Life Science) was performed at pH 8.5 (IgG) or pH 9.0 (IgG Fab) as described previously (2).

**$\beta$ 1 integrin Cyto domain peptides and pull-down assay.** Four overlapping peptides based on the cytoplasmic sequence of human  $\beta$ 1 integrin were synthesized and biotinylated at the N terminus (see Fig. 2). For *in vitro* pull-down assays, cell extracts (obtained by lysing transfected cells with a modified radioimmunoprecipitation assay [RIPA] buffer containing 1% [wt/vol] *n*-octyl- $\beta$ -D-glucopyranoside) containing either full-length GFP-PKC $\alpha$  protein or one of the GFP-PKC $\alpha$  RD construct proteins were left to tumble overnight at 4°C with various  $\beta$ 1 integrin Cyto domain peptides on beads (a 1-mg/ml peptide solution was used to precoat streptavidin-coupled agarose beads [Sigma] for 1 h at 4°C, which were then washed extensively with cell extraction buffer). The GFP-PKC $\alpha$ /peptide complexes were then washed three times with RIPA buffer and once with Tris-saline buffer (pH 7.4) and subsequently resuspended in Laemmli sample buffer and analyzed by immunoblotting using an anti-GFP rabbit antiserum (Clontech). The conformational requirement for PKC $\alpha$  to bind to the  $\beta$ 1 integrin Cyto domain peptides *in vitro* was investigated by preincubating the cell extract containing the full-length PKC $\alpha$  protein or RD PKC $\alpha$  protein with an equal volume of RIPA buffer containing mixed phosphatidylserine (PS) and phorbol 12-myristate 13-acetate (TPA) micelles (2.5 mg of PS per ml and 2.5  $\mu$ g of TPA sonicated prior to its addition to cell extract). For the GST-PKC $\alpha$  pull-down assays, various GST-PKC $\alpha$  constructs (expressed in *Escherichia coli* and eluted off glutathione-Sepharose beads) were used instead of detergent cell extracts for the binding to  $\beta$ 1 integrin Cyto domain peptide GK21.

**TUNEL assay for detection of apoptosis.** Cells were harvested and fixed in 2% paraformaldehyde. Terminal deoxynucleotidyltransferase (TdT)-mediated dUTP-biotin nick end labeling (TUNEL) assay was performed according to the manufacturer's protocol (Promega). Apoptosis was detected using fluorescein-linked dUTP. Samples were analyzed by flow cytometry to determine the percentage of apoptotic cells within the population.

**Cell surface biotinylation, immunoprecipitation, and Western blotting.**  $\beta$ 1-null GD25 cells were transfected with (i) a GFP-PKC $\alpha$  RD domain construct with the  $\beta$ 1-pECE plasmid or (ii) the IL-2R- $\beta$ 1 integrin chimera alone. Cell surface proteins were biotinylated as described previously using the Amersham protein biotinylation module (Amersham Pharmacia), and cells were lysed in buffer containing 1% Brij 96 (34).  $\beta$ 1 integrin was immunoprecipitated from the detergent-soluble cell fraction using an anti- $\beta$ 1 rabbit serum (a kind gift of J. Ivaska, Imperial Cancer Research Fund). An anti- $\beta$ 1 integrin MAb (clone DF7; Affiniti UK) was used for Western blotting. The immunoprecipitates were denatured in sample buffer, separated on an 8% polyacrylamide gel under reducing conditions, and transferred electrophoretically to a polyvinylidene difluoride membrane. Blots were then probed with either a rabbit anti-GFP antiserum or antiserum directed against the C terminus of PKC $\alpha$ . The membrane was stripped and reprobed with horseradish peroxidase (HRP)-conjugated streptavidin to detect biotinylated proteins.

**Dunn chamber chemotaxis assays.** Chemotaxis of cells was assessed using time-lapse microscopy of cell behavior in response to a phorbol dibutyrate (PDBu) gradient within a Dunn chemotaxis chamber (Weber Scientific International, Ltd., Teddington, United Kingdom) (36). Briefly, the chamber consists of two circular wells separated by a platform which lies 20  $\mu$ m below the upper surface of the slide. The inner well was filled with control medium, while the outer well contained medium with 1  $\mu$ M PDBu. The coverslip was then placed over the chamber and sealed with wax around the edges, allowing the establishment of a diffusion gradient across the platform distance. Cells within one field of the platform were then filmed over 16 h with the outer well edge at the top (0°) of the image using a 10 $\times$  objective.

**Cell tracking and statistical analysis of migration.** Analysis of both directional ( $\Delta y$ ) and speed data was performed by manually tracking cells within each field over the sequence of time-lapse digital images (Motion Analysis software; Kinetic Imaging, Merseyside, United Kingdom). The resultant cell trajectories were converted into a single angle, and the points were then pooled and summarized in a circular histogram showing the number of cell directions lying within 18° intervals (35). Comparisons between different groups of experiments were made by applying analysis of variance (ANOVA) to both directional and cell mean speed tracking data (35). *P* values of <0.05 indicate significant clustering of cell directions around the gradient (upwards) and therefore demonstrate positive chemotaxis.

**Transwell chamber migration analysis.** MDA-MB231 cells were transiently infected with media from Phoenix packaging cells (Stanford University) containing intact retrovirus encoding myc-tagged GK  $\beta$ 1 peptide or scrambled equivalent or the pBabe vector alone. Infection efficiency was checked using parallel fixed cultures stained with anti-myc antibodies. At 48 h postinfection, 231 cells were trypsinized and replated into six-well (24-mm-diameter insert) Transwell plates at a concentration of  $5 \times 10^5$  cells/well. The bottom well in each case contained serum-free media supplemented with 1  $\mu$ M PDBu or 100 ng of EGF per ml, except for control wells, which contained media alone. Cells were then incubated for 8 h at 37°C, trypsinized separately from each top and bottom well, centrifuged, and fixed in 4% paraformaldehyde. Total numbers of cells in each chamber were then counted using a CASY-1 cell counter (Sharfe System GmbH, Germany).

**FLIM measurements.** A detailed description of the fluorescence lifetime imaging microscopy (FLIM) apparatus used for fluorescence resonance energy transfer (FRET) determination in this work can be found elsewhere (19, 24). This instrument performs phase- and modulation-based imaging fluorimetry by microscopy. All images were taken using a Zeiss Plan-APOCHROMAT 100 $\times$ /1.4-numerical-aperture (NA) phase 3 oil objective, and the homodyne phase-sensitive images were recorded at a modulation frequency of 80.224 MHz.

**Confocal microscopy.** Confocal images were acquired with a confocal laser scanning microscope (model LSM 510; Carl Zeiss Inc.) equipped with both 40 $\times$ /1.3Plan-Neofluar and 63 $\times$ /1.4Plan-APOCHROMAT oil immersion objectives. Each image represents a two-dimensional projection of two or three slices in the *z* series, taken across the cell at middepth at 0.2- $\mu$ m intervals.

**Video microscopy.** Cells were observed at 37°C, after the addition of PDBu (1  $\mu$ M), on an inverted microscope (Axiovert 200 TV; Carl Zeiss) equipped for epifluorescence and phase-contrast microscopy, using 63 $\times$ /NA 1.4 Plan-Neofluar. Data were acquired with a back-illuminated, cooled charge-coupled device camera (Orca ER) from Hamamatsu driven by AQM-NT-MC powerful multichannel, time-lapse imaging core software (Kinetic Imaging, Ltd.) and stored as 16-bit digital images. Times between frames were 5 s.

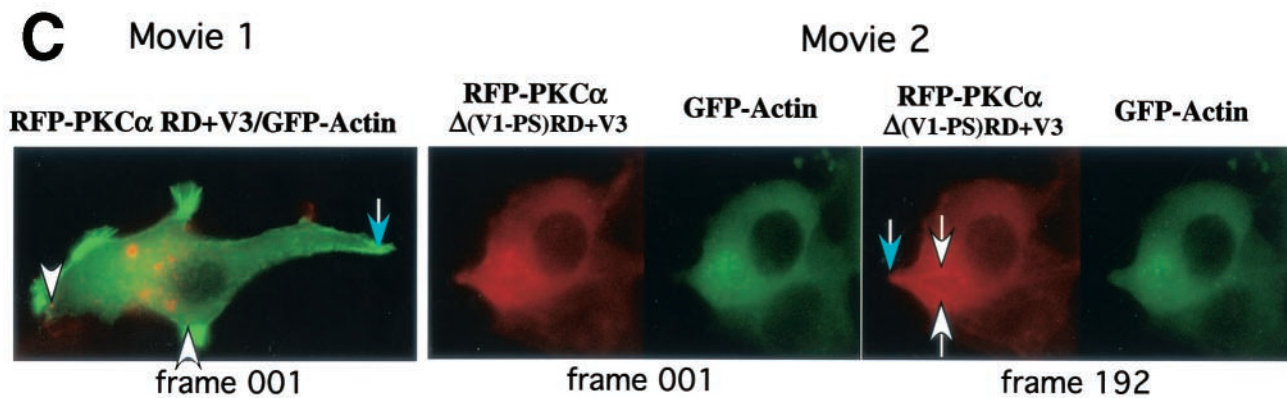
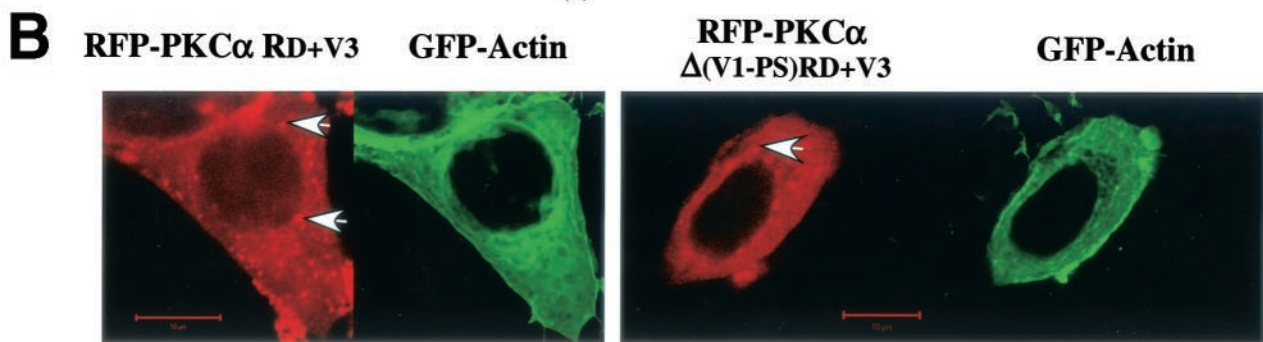
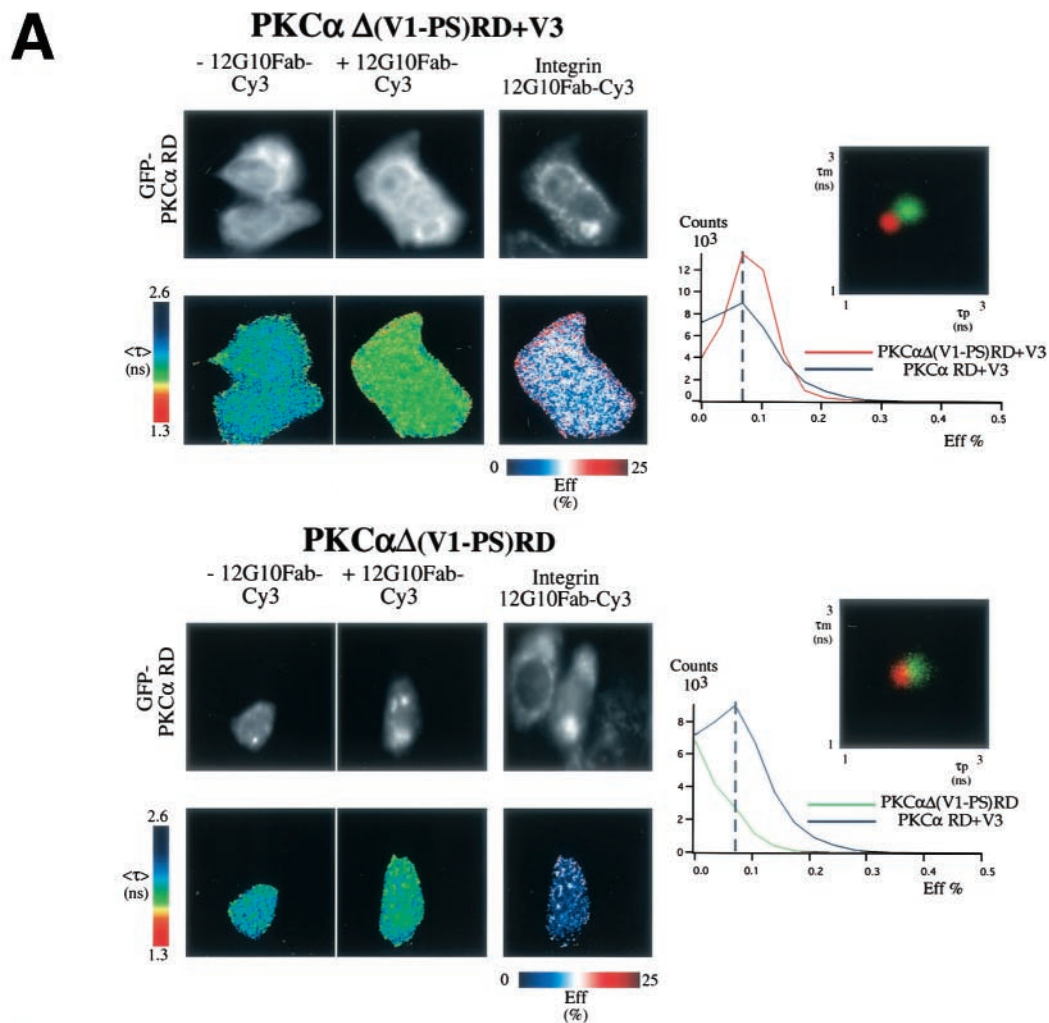
## RESULTS

**PKC $\alpha$ -induced directional migration requires the presence of the V3 hinge domain.** To characterize the molecular determinants for PKC $\alpha$ -mediated MCF-7 cell migration (16), cells transfected with different GFP-PKC $\alpha$  RD constructs or with empty vector control were exposed to a PDBu gradient in a Dunn motility chamber. Transient expression of full-length GFP-PKC $\alpha$ , but not GFP alone, conferred the ability to migrate towards the chemotactic gradient with significant directionality (*P* < 0.001 by ANOVA) (Fig. 1A). A control gradient of the biologically inactive 4 $\alpha$ -phorbol at the same concentration showed no chemotactic effect (data not shown). Cells expressing two RD constructs containing the V3 hinge region, GFP-PKC $\alpha$  RD+V3 and GFP- $\Delta$ (V1-PS)RD+V3 (V, variable domain; PS, pseudosubstrate site) also exhibited significant directionality towards the PDBu gradient (*P* < 0.001 and *P* < 0.01, respectively), indicating that the first variable region (V1), the pseudosubstrate site, and the catalytic domain are not required for PKC $\alpha$ -driven directional cell movement. However, cells expressing the GFP- $\Delta$ (V1-PS)RD construct, which does not contain the V3 region, displayed no significant directionality. Untransfected MCF-7 cells (with no detectable endogenous PKC $\alpha$ ) also showed no significant directional motility towards the PDBu gradient. Together, these data indicate that the hinge region of PKC $\alpha$  contains the molecular determinant for directional cell motility.

Previously we showed that MCF-7 cells transiently expressing a full-length PKC $\alpha$ -GFP exhibited a significant increase in haptotactic migration towards  $\beta$ 1, but not  $\alpha$ V, substrates (16). Figure 1B shows that the directionality of cell movement conferred by transiently expressing the V3-containing GFP-PKC $\alpha$  RD construct can also be eliminated specifically by an anti- $\beta$ 1, but not anti- $\alpha$ V, integrin blocking antibody, in keeping with our previously published results. Furthermore, directional cell movement of cells expressing GFP-PKC $\alpha$  RD+V3, despite the absence of a catalytic domain, was sensitive to inhibition by bisindolylmaleimide (Fig. 1C).

**The V3 region of PKC $\alpha$  is required for PKC $\alpha$ - $\beta$ 1 integrin association.** We previously reported that upon TPA treatment, the GFP-PKC $\alpha$  RD+V3 protein becomes complexed to activated  $\beta$ 1 integrin (16). In order to characterize the binding sites further, four N-terminally biotinylated, overlapping peptides based on the cytoplasmic sequence of human  $\beta$ 1 integrin were synthesized. Of these, GK21, which contained both Cyto-2 and Cyto-3 domains, was most effective in pulling down full-length GFP-PKC $\alpha$  (WT) protein, expressed in MCF-7 cells (Fig. 2A). Figure 2B shows that this peptide can associate with GFP-PKC $\alpha$  WT, GFP-PKC $\alpha$  RD+V3, and GFP-PKC $\alpha$   $\Delta$ (V1-PS)RD+V3, but not with GFP- $\Delta$ (V1-PS)RD in vitro in an PS- or TPA-dependent manner. The efficiency of PKC $\alpha$   $\Delta$ (V1-PS)RD+V3 pulldown by GK21 in vitro was noted to be lower than that of PKC $\alpha$  RD+V3, suggesting the V1-PS domain might play an additional regulatory role in PKC $\alpha$ - $\beta$ 1 integrin association.

The requirement of the V3 hinge region for PKC $\alpha$ - $\beta$ 1 integrin association was confirmed in vivo by the detection of FRET between 12G10-positive, activated  $\beta$ 1 integrins and GFP-PKC $\alpha$  RD+V3 and GFP-PKC $\alpha$   $\Delta$ (V1-PS)RD+V3 but not GFP-PKC $\alpha$   $\Delta$ (V1-PS)RD in TPA-stimulated cells. These



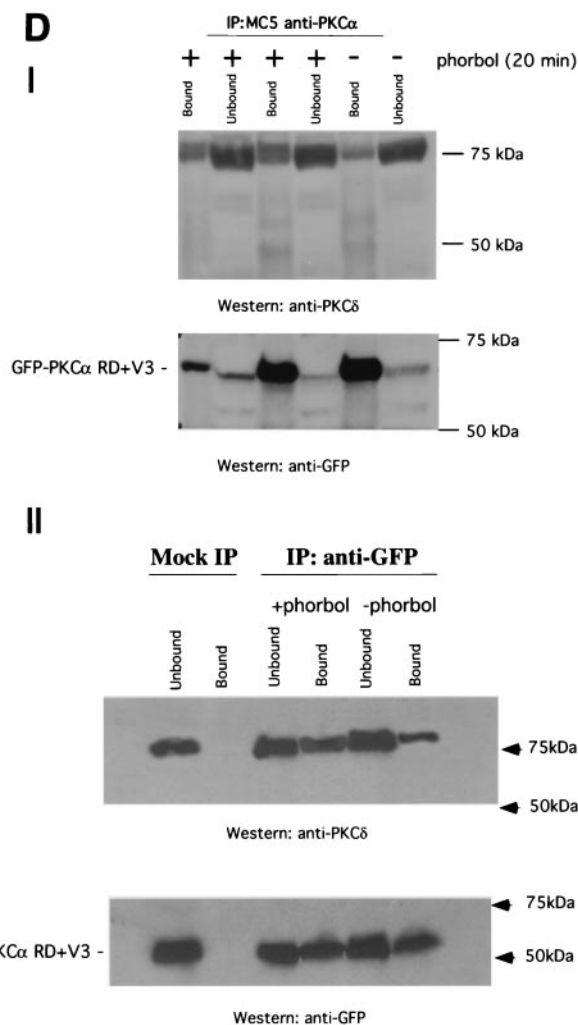


FIG. 3. Structural requirement for PKC $\alpha$  RD in  $\beta$ 1 integrin association and its localization in MCF-7 cells. (A) MCF-7 cells were transiently transfected with various GFP-tagged PKC $\alpha$  RD constructs [GFP- $\Delta$ (V1-PS)RD+V3, GFP- $\Delta$ (V1-PS)RD, and GFP-PKC $\alpha$  RD+V3]. Cells were stimulated with TPA (400 nM) and fixed after 20 min of incubation at 37°C and then either left as controls or stained with Mab 12G10 Fab (+12G10 Fab-Cy3). The fluorescence images from the donor (GFP-PKC $\alpha$  RD) and acceptor (Integrin 12G10 Fab-Cy3) are shown.  $\langle\tau\rangle$  is the average of  $\tau_p$  and  $\tau_m$ , and its pseudocolor scale applies to all four lifetime maps. The FRET efficiency (Eff) pseudocolor plots apply only to the + 12G10 Fab-Cy3 lifetime maps (Eff =  $1 - \tau_{DA}/\tau_D$ , where  $\tau_{DA}$  is the lifetime map of the donor in the presence of acceptor and  $\tau_D$  is the average lifetime of the donor in the absence of acceptor [average of the mean  $\langle\tau\rangle$  of at least four GFP-PKC RD alone control cells]). The pixel count-versus-FRET efficiency graphs to the right summarize the difference between the different RD constructs in their capacities to bind activated  $\beta$ 1 integrins [GFP-PKC $\alpha$  RD+V3 (blue trace), GFP-PKC $\alpha$   $\Delta$ (V1-PS)RD+V3] (red trace), and GFP-PKC $\alpha$   $\Delta$ (V1-PS)RD (green trace)]. Results for GFP-PKC $\alpha$  RD+V3 were similar to those published previously using the same assay (16) and summarized in the pixel count-versus-FRET efficiency graphs for comparison. The cumulative lifetimes of GFP-PKC $\alpha$  donor alone (green) and that measured in the presence of the acceptor fluorophore (red) ( $n = 5$ ) are plotted on the two-dimensional graphs in the inserts shown to the right. (B) Confocal images of unstimulated, paraformaldehyde-fixed MCF-7 cells coexpressing RFP-PKC $\alpha$   $\Delta$ (V1-PS)RD+V3 or RFP-PKC $\alpha$  RD+V3 and GFP-actin. Bars = 10  $\mu$ m. (C) Still images from supplementary movies 1 and 2 of live MCF-7 cells coexpressing RFP-PKC $\alpha$  RD+V3 (movie 1) or RFP-PKC $\alpha$   $\Delta$ (V1-PS)RD+V3 (movie 2) and GFP-actin, simulated with

data are illustrated in Fig. 3 and summarized by the pixel count-versus-FRET efficiency graphs to the right in Fig. 3A. The extent of complex formation between activated  $\beta$ 1 integrin and GFP-PKC $\alpha$   $\Delta$ (V1-PS)RD, which differs from GFP-PKC $\alpha$   $\Delta$ (V1-PS)RD+V3 by lacking the V3 domain was significantly lower. This implies that the variable region V3 of PKC $\alpha$  is required for PKC $\alpha$ - $\beta$ 1 integrin association upon activation.

The intensified light images generated by the microchannel plate detector in our wide-field fluorescence lifetime microscope are not of sufficient resolution to determine whether RD constructs such as PKC $\alpha$   $\Delta$ (V1-PS)RD+V3, which lack the V1-PS domain but retain the capacity to interact with plasma membrane- or vesicle-associated  $\beta$ 1 integrin, could translocate to the membrane compartment efficiently in response to phorbol treatment. However, confocal microscopy revealed that while the majority of PKC $\alpha$   $\Delta$ (V1-PS)RD+V3 (RFP tagged to allow a simultaneous visualization of PKC $\alpha$  with GFP-actin in live cells stimulated with phorbol ester) appeared to be cytosolic, a subpopulation was associated with a vesicular compartment (Fig. 3B). In contrast, the majority of RFP-PKC $\alpha$  RD+V3 was membrane or vesicle bound, in agreement with previously published findings indicating a plasma membrane targeting role for the V1-PS domain in conventional PKCs (18, 27). The vesicle-bound subpopulation of PKC $\alpha$   $\Delta$ (V1-PS)RD+V3, like PKC $\alpha$  RD+V3, was shown to actively traffic directionally to the leading edge as the cell protruded in response to PDBu stimulation. These extending cell processes are characterized by an actin-rich ruffling membrane and targeted by actin-enriched membrane vesicles (Fig. 3C and supplementary movies 1 and 2). Western blot analysis of immunoprecipitates from transfected MCF-7 cells, which do not contain endogenous PKC $\alpha$ , suggested that endogenous PKC $\delta$  was also recruited, in a PDBu-responsive manner, to the PKC $\alpha$  RD+V3-containing signaling complex. The proportional recovery of PKC $\delta$  in the anti-PKC $\alpha$  immunoprecipitate, corrected for any difference in the efficiency of precipitation as

PDBu (1  $\mu$ M). Frame 001 corresponded to 1 min (movie 1) and 3 min (movie 2) after the addition of PDBu (1  $\mu$ M) to tissue medium, respectively. Time-lapse series were taken as described in Materials and Methods. During filming, from time to time, the microscope had to be manually adjusted to reestablish the focus, which was less stable with high-power objectives even though the temperature was maintained at 37°C. The white arrows point to RFP-PKC $\alpha$  RD+V3-enriched vesicles that moved in and out of actin-rich cell ruffles (movie 1) and RFP-PKC $\alpha$   $\Delta$ (V1-PS)RD+V3-enriched vesicles that trafficked in streams directionally to the leading edge as the cell protruded in response to PDBu stimulation (movie 2). The blue arrows point to the tail of the cell with little or no RFP-PKC $\alpha$  RD+V3 vesicle traffic (movie 1) and a PDBu-induced cell protrusion (movie 2). (D) Panel I shows the coprecipitation of GFP-PKC $\alpha$  RD+V3 with PKC $\delta$ , in response to stimulation with phorbol ester (1  $\mu$ M PDBu) (+). All the bound proteins on the protein G bead (Bound) and one-fifth of the unbound proteins left in the cell extract supernatant after the first centrifugation postprecipitation (Unbound) were loaded. The blot containing the anti-PKC $\alpha$  (Mab MC5) immunoprecipitates was first probed with a rabbit anti-PKC $\delta$  polyclonal antibody and then stripped and reprobed with an anti-GFP rabbit serum (Clontech). Duplicates of the +PDBu samples were run. The positions of the molecular mass markers are shown. Panel II is a repeat of the experiment in panel I, with a mock immunoprecipitation (IP) control (i.e., immunoprecipitation with a preimmune serum); immunoprecipitation of GFP-PKC $\alpha$  RD+V3 was performed with a rabbit anti-GFP serum.

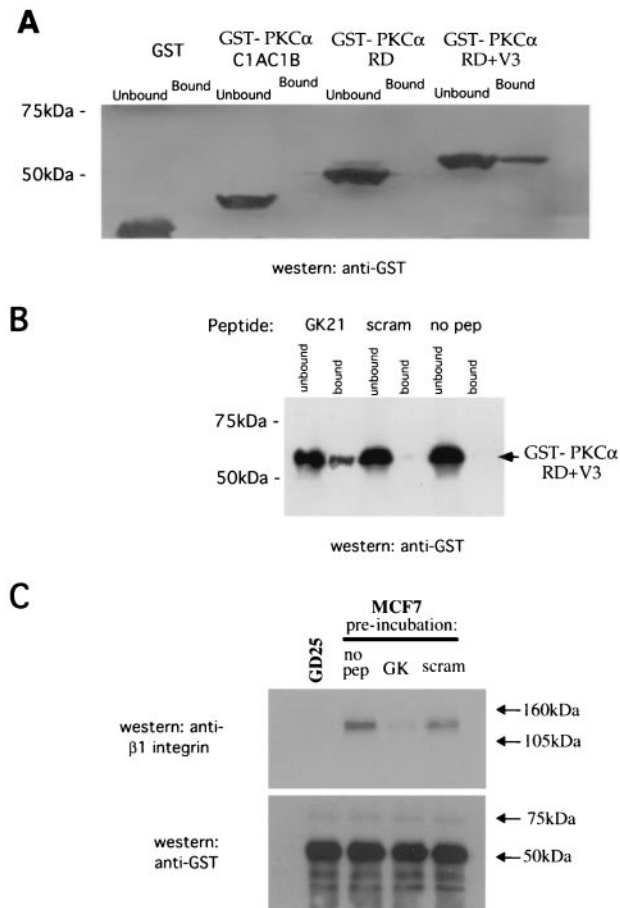


FIG. 4. Direct association of purified GST-PKC $\alpha$  RD with a  $\beta$ 1 integrin cytoplasmic peptide in vitro. (A) In an in vitro pull-down assay (described in Materials and Methods), the binding of GST-PKC $\alpha$  RD+V3, GST-PKC $\alpha$  RD, PKC $\alpha$  C1AC1B (aa32-156), or GST alone to the  $\beta$ 1 integrin Cyto-2- and Cyto-3-containing peptide GK was compared. For each sample, all of the peptide-bound GFP-PKC $\alpha$  (Bound) was run alongside one-fifth of the corresponding supernatant containing unbound proteins (Unbound). (B) Binding of GST-PKC $\alpha$  RD+V3 to streptavidin-agarose beads coated with GK, but not its scrambled equivalent (scram) or no-peptide (no pep) control. (C) GST-PKC $\alpha$  RD+V3 on glutathione beads were not treated (no peptide [no pep]) or preincubated with free GK peptide or its scrambled equivalent (scram) (1 mg/ml) for 1 h at 4°C, washed with cell extraction buffer, and then tumbled with cell extracts from either MCF-7 or  $\beta$ 1 integrin-null GD25 cells. The bound fraction was then analyzed for  $\beta$ 1 integrin and GST-PKC $\alpha$  contents by immunoblotting.

shown by the anti-GFP blot, was increased by approximately 84 and 85% following PDBu treatment (Fig. 3D, panels I and II, respectively). We also demonstrated a direct in vitro interaction between purified, bacterially expressed GST-PKC $\alpha$  RD+V3, but not GST-PKC $\alpha$  RD or PKC $\alpha$  C1AC1B (aa32-156), and the  $\beta$ 1 integrin Cyto-2- and Cyto-3-containing peptide GK21 (Fig. 4A), further substantiating the requirement of the V3 domain for the direct association between PKC $\alpha$  and  $\beta$ 1 integrin. We did not observe any binding of GST-PKC $\alpha$  RD+V3 to streptavidin-agarose beads coated with the scrambled GK21 peptide or to the no-peptide control (Fig. 4B). Preincubation of GST-PKC $\alpha$  RD+V3 on glutathione beads with free GK peptide, not its scrambled equivalent, eliminated

its ability to associate with  $\beta$ 1 integrin from MCF-7 cell extract in vitro (Fig. 4C)

**Coimmunoprecipitation of full-length human  $\beta$ 1 integrin/IL-2R- $\beta$ 1 integrin chimera with human PKC $\alpha$  in  $\beta$ 1-null GD25 cells.** To examine the interaction between PKC $\alpha$  and  $\beta$ 1 integrin in vivo, surface-biotinylated GD25 ( $\beta$ 1-null) cells were cotransfected with a full-length  $\beta$ 1A integrin-pECE with various GFP-tagged PKC $\alpha$  RD constructs. WT GFP-PKC $\alpha$ , GFP-PKC $\alpha$  RD+V3, and GFP-C2V3, but not GFP PKC $\alpha$ - $\Delta$ (V1-PS)RD or GFP-PKC $\alpha$  RD, were coprecipitated with  $\beta$ 1 integrin, reiterating the requirement of the V3 domain for the direct association between PKC $\alpha$  and  $\beta$ 1 integrin (Fig. 5A). In addition, a fusion chimera between the cytoplasmic tail of  $\beta$ 1 and both the transmembrane and extracellular domains of IL-2R was transiently expressed (14). This construct does not dimerize with functional integrin  $\alpha$  subunits and was therefore used to examine the unique contribution of the  $\beta$  chain to PKC/integrin complex formation. This construct was expressed in a  $\beta$ 1-null cell line, GD25, in which cell surface proteins were biotinylated for subsequent detection in anti-IL-2R immunoprecipitates by probing with HRP-conjugated streptavidin. The association of IL-2R-WT  $\beta$ 1A integrin chimera with endogenous PKC $\alpha$  in GD25 cells was more efficient than that of the IL-2R- $\beta$ 1A (aa757-796) which lacks the Cyto-3 subdomain (Fig. 5B). IL-2R- $\beta$ 1A (aa757-784), which lacks both the Cyto-2 and Cyto-3 subdomains, was not coprecipitated with endogenous PKC $\alpha$  (Fig. 5B). Therefore, both Cyto-2 and Cyto-3 amino acid clusters are involved in integrin/PKC $\alpha$  complex formation.

**A 12-amino-acid motif within the PKC $\alpha$  V3 domain contains both the  $\beta$ 1 integrin binding site and the determinant for directional cell movement.** To characterize further the integrin binding site within the PKC $\alpha$  V3 domain, the peptide pull-down assay in Fig. 2B was repeated using various GFP-tagged PKC $\alpha$  V3 domain truncation constructs expressed in MCF-7 cells (Fig. 6A). There was a pronounced reduction (between 73 to 83%) in GK21 binding between the aa1-313 and aa1-325 truncations, indicating that a 12-amino-acid motif (G<sup>314</sup>NKVISPSEDRK<sup>325</sup>) is involved in integrin binding (Fig. 6B). The integrity of the aa1-313 protein construct was confirmed by its immunodetection with an anti-PKC $\alpha$  MAb which recognizes the LRQKFEKAK (aa301-309) epitope (data not shown). Next, we expressed the same PKC constructs in  $\beta$ 1 integrin-null GD25 cells, and an in vivo association between transfected full-length  $\beta$ 1A integrin and the GFP-PKC $\alpha$  V3 domain truncation aa1-325 or aa1-337, but not aa1-301, was detected reproducibly by coprecipitation ( $n = 3$ ) (Fig. 6C). Binding of truncation construct aa1-313 to  $\beta$ 1A integrin was significantly impaired in comparison to that of aa1-325 (mean 82% reduction,  $P < 0.001$ ,  $n = 3$ ). There was no statistical difference between aa1-325 or aa1-337 in terms of  $\beta$ 1A integrin binding ( $P = 0.256$ ,  $n = 3$ ). The effects of expressing the same PKC $\alpha$  V3 domain truncation constructs on directional cell motility were examined in the Dunn chamber. MCF-7 cells expressing the V3 domain truncation aa1-325 or aa1-337, but not aa1-301 or aa1-313, were able to migrate directionally towards a PDBu gradient (Fig. 6D).

**Elimination of PKC $\alpha$ - and EGF-induced chemotaxis of breast carcinoma cells by a  $\beta$ 1 integrin cytoplasmic sequence.**



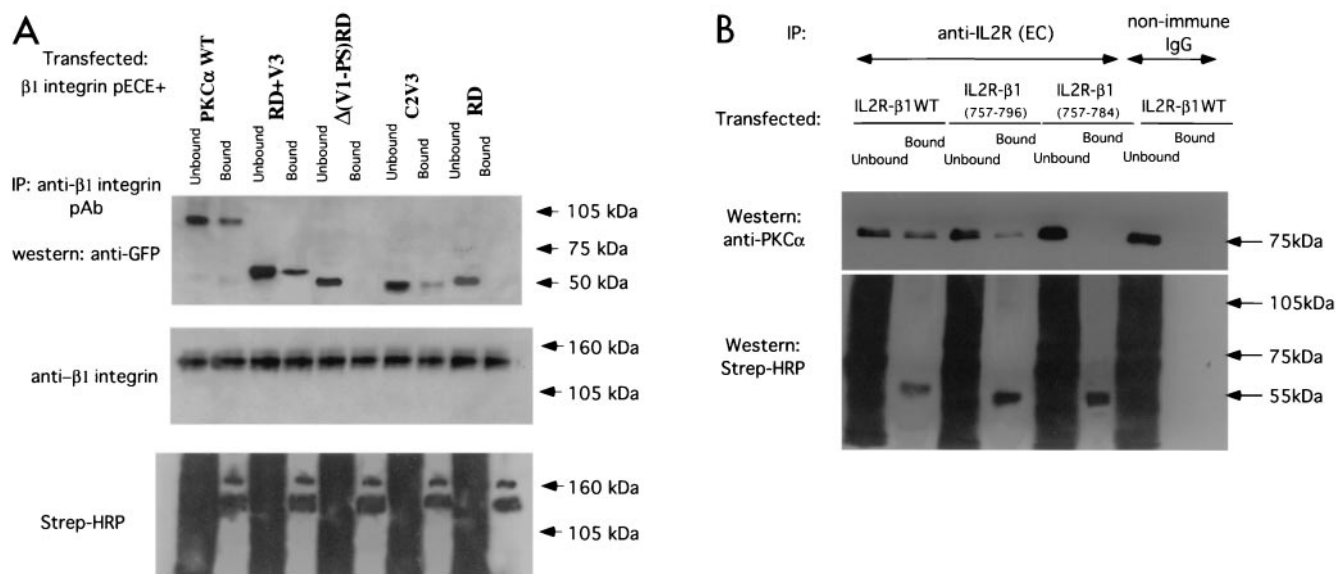


FIG. 5. Binding site mapping by coimmunoprecipitation of human  $\beta 1$  integrin/IL-2R- $\beta 1$  integrin chimera with PKC $\alpha$  in  $\beta 1$ -null GD25 cells. (A) Coprecipitation of  $\beta 1A$  integrin (immunoprecipitated with a rabbit polyclonal antiserum against human  $\beta 1$  integrin) with GFP-PKC $\alpha$  WT, GFP-PKC $\alpha$  RD+V3, and GFP-PKC $\alpha$  C2V3, but not with GFP-PKC $\alpha$   $\Delta(V1-PS)RD$ , or GFP-PKC $\alpha$  RD, as detected by an anti-GFP antibody. The proteins were from cell surface-biotinylated GD25 cells which were cotransfected with a full-length untagged  $\beta 1A$  integrin-pECE and various GFP-tagged PKC $\alpha$  RD constructs. All the bound proteins on the protein G bead (Bound) and one-fifth of the unbound proteins left in the cell extract supernatant after the first centrifugation after precipitation (Unbound) were loaded. The blot containing the anti-integrin immunoprecipitates was stripped and reprobed with an anti- $\beta 1$  integrin MAb; a similarly prepared duplicate blot was probed with HRP-conjugated streptavidin. Two predominant biotinylated surface proteins were immunoprecipitated using the anti- $\beta 1$  polyclonal antibody, representing the  $\beta 1$  integrin  $\alpha/\beta$  heterodimer (the lower band comigrates with the  $\beta$  chain detected by the anti- $\beta 1$  integrin MAb). Positions of the approximate molecular mass markers are shown. (B) Coprecipitation of IL-2R-WT  $\beta 1A$  integrin or its truncation constructs (containing the extracellular [EC] and transmembrane [TM] domains of IL-2R and the intracellular [IC] portion of  $\beta 1A$ ) with endogenous PKC $\alpha$ , as detected by a rabbit polyclonal antiserum against PKC $\alpha$ . The proteins were from GD25 cells transfected with an IL-2R- $\beta 1A$  integrin (aa757-803, WT or aa757-796 or aa757-784) chimera. All the bound proteins on the protein G bead (Bound) and one-fifth of the unbound proteins left in the cell extract supernatant after the first centrifugation postprecipitation (Unbound) were loaded. The blot was stripped and reprobed with HRP-conjugated streptavidin (Strep-HRP).

We used two different approaches to investigate the role of the  $\beta 1$  cytoplasmic tail in PKC $\alpha$ -induced cell motility. First, a peptide derived from the  $\beta 1A$  cytoplasmic domain (aa783-803; GENPIYKSAVTTVVNPKYEGK) (GK21) was manufactured by chemical synthesis in tandem with the *antennapedia* third helix (residues 43 to 58) sequence (RQIKIWFQNR RMKWKK) and rhodaminated to allow visualization (ANT-GK21). Full-length GFP-PKC $\alpha$  was shown to associate in vitro with ANT-GK21 peptide but not with a scrambled control peptide (GTAKINEPYSVTPVYGEKNKVRQIKIWFQNR RMKWKK) (Fig. 7A). ANT-GK21 was shown to abolish the directionality of PKC-driven cell migration (towards a PDBu gradient) as well as EGF-induced chemotaxis in our Dunn chamber assays (Fig. 7B and C). These data suggest that the Cyto-2- and Cyto-3-containing  $\beta 1$  peptide interferes with the interaction between endogenous  $\beta 1$  integrin and PKC $\alpha$ , exerting a dominant negative effect upon the migratory phenotype of these cells.

In order to work towards a more controlled peptide delivery system, we generated retroviral constructs encoding the  $\beta 1$  cytoplasmic peptide GK21 sequence or its scrambled equivalent, tagged with the myc epitope to allow subsequent detection in cells. These retroviral constructs were introduced into MDA-MB231 cells, and subsequent effects on motility were analyzed in a Transwell chemotaxis assay. At 48 h postinfect-

ion, approximately 70% of cells were shown to express the myc-tagged sequence, as shown by MAb staining (data not shown). Cells expressing either the scrambled sequence or the pBABE empty vector exhibited migratory capacities similar to that of uninfected cells (Fig. 8). By contrast, infected cells expressing the  $\beta 1$  cytoplasmic GK21 sequence demonstrated a dramatic reduction in chemotaxis towards PDBu (90% reduction, in three independent, double-blind assays;  $P < 0.001$  by ANOVA) (Fig. 8A) or EGF (75% reduction, in two independent, double-blind assays;  $P < 0.001$  by ANOVA) (Fig. 8B). Potential cell toxicity effects were assessed using TUNEL. Figure 9 demonstrates that there was no significant cell death associated with any of the retroviral constructs.

## DISCUSSION

Published studies of human breast tumor cells treated with anti- $\beta 1$  integrin blocking antibodies in three-dimensional culture and nude mice demonstrated a role for  $\beta 1$  integrins in the development of a malignant phenotype expressed as an increase in tumorigenicity and invasiveness in vivo (29). Previously we have shown that PKC $\alpha$  physically associates with  $\beta 1$  integrin and that increased PKC $\alpha$  expression promotes the migration of breast cancer cells. We therefore sought to (i) identify the molecular determinant on PKC $\alpha$  that is critical for

conferring directional cell motility, (ii) characterize the minimal sequences required for the interaction on both PKC $\alpha$  and the  $\beta$ 1 integrin, and (iii) determine whether a site-directed perturbation of the PKC $\alpha$ - $\beta$ 1 integrin complex would affect the directional motility response of breast cancer cells.

We report that the RD of PKC $\alpha$ , or more specifically a 12-amino-acid region (aa313-325) within the V3 hinge region, is a key site for determining the directionality of PKC $\alpha$ -driven,  $\beta$ 1 integrin-dependent cell migration. This activity is independent of the PKC $\alpha$  catalytic domain. The V3 domain is also required for PKC- $\beta$ 1 integrin association both in vitro and in intact cells. Very little is known about the function of this domain in PKC. The minimum sequence responsible for the cytoplasmic sequestration of PKC $\alpha$  is believed, however, to be contained in a region within C2-V3 (27). Phorbol ester stimulation is known to increase the locomotory activity and haptotactic responses of colon and breast carcinoma cells (16, 21). Importantly, the RD (with the V3 hinge) of PKC $\alpha$ , in the absence of the kinase domain, is shown here to be sufficient for the induction of cell polarization and subsequent directed cell movement towards a phorbol ester gradient. However, the kinase domain is required during the haptotactic transmigration of transfected MCF-7 cells towards  $\beta$ 1 integrin substrates (16). This model was designed to examine cancer cell migration in a different context where PKC $\alpha$  activation is stimulated by integrin ligation (not phorbol ester) and appears to require a full-length protein; it can be surmised that other PKCs are not activated under these circumstances in a manner sufficient to support the action of the RD+V3 domain. PKC $\alpha$  RD+V3-expressing MCF-7 cells were also unable to migrate towards an EGF gradient (M. Parsons and T. Ng, unpublished data), emphasizing the kinase domain requirement in this context. The directionality of cell movement conferred by transiently expressing the V3-containing GFP-PKC $\alpha$  RD construct can be specifically eliminated by an anti- $\beta$ 1, but not anti- $\alpha$ V, integrin blocking antibody. This is in keeping with our finding that the V3 domain contains the prerequisite binding sequence for targeting PKC $\alpha$  to  $\beta$ 1 integrin. Integrin receptors are cell polarity proteins involved in a polarized endocytic cycle during cell movement (5, 11, 12, 16). We propose that  $\beta$ 1 integrin as a binding protein that interacts specifically with the V3 domain may serve to direct PKC to the leading edge, where downstream events such as actin nucleation and polymerization can be triggered (25, 26). Indeed, our time-lapse experiments (movies 1 and 2) showed that two of our V3-containing PKC $\alpha$  RD constructs, in the absence of the kinase domain, can actively traffic directionally to the leading edge (actin-rich ruffling membrane) as the cell protrudes in response to PDBu stimulation. Additionally, we observed that endogenous PKC $\delta$  was also recruited, in response to PDBu stimulation, to the PKC $\alpha$  RD+V3-containing signaling complex, which would explain the sensitivity of PKC $\alpha$  RD+V3-directed migration to inhibition by bisindolylmaleimide.

The association of PKC $\alpha$  with the  $\beta$ 1 integrin cytoplasmic domain is direct, as shown by (i) the binding of purified GST-PKC $\alpha$  fusion proteins to the  $\beta$ 1 tail-derived peptide GK21, (ii) the association in vivo between an IL-2R- $\beta$ 1 integrin chimera and endogenous PKC $\alpha$  in the absence of an associated integrin  $\alpha$  chain, and (iii) the demonstration of FRET by FLIM between V3-containing GFP-PKC $\alpha$  RD constructs and Cy3-la-

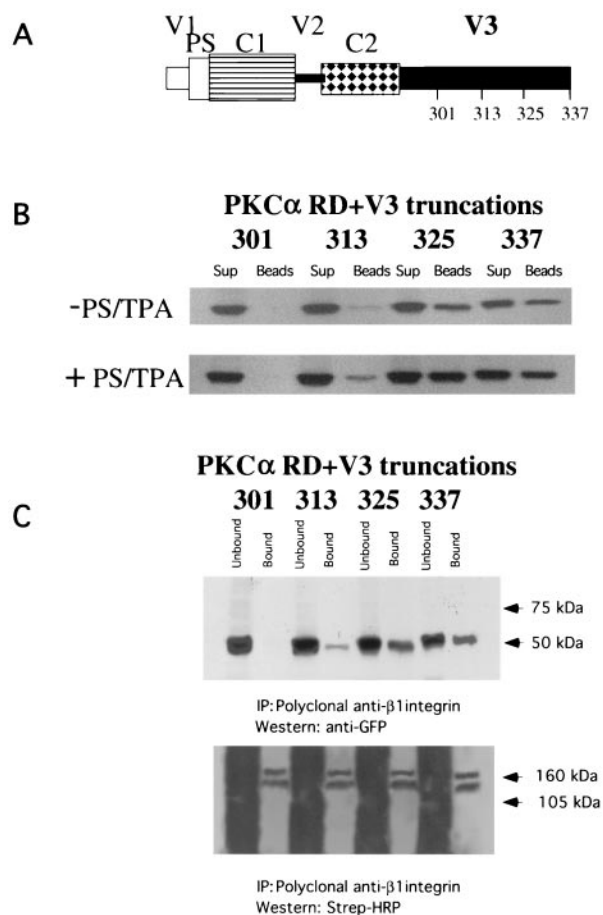


FIG. 6. Identification of a 12-amino-acid region within the third variable domain (V3) of PKC $\alpha$  to contain both the lipid-dependent binding site for  $\beta$ 1 integrin and molecular determinant for directional cell movement. (A) Schematic representation of various PKC $\alpha$  RD+V3 truncation constructs. (B) Complex formation between various GFP-tagged PKC $\alpha$  V3 domain truncation constructs expressed in MCF-7 cells (in the presence [+] and absence [-] of PS and TPA): 301 (aa1-301), 313 (aa1-313), 325 (aa1-325), and 337 (aa1-337), with the biotinylated GK21 peptide as described in the legend to Fig. 2B. (C) Coprecipitation of  $\beta$ 1A integrin (immunoprecipitated [IP] with a rabbit polyclonal antiserum against human  $\beta$ 1 integrin) with PKC $\alpha$  325 (aa1-325) and 337 (aa1-337), as detected by an anti-GFP antibody. The proteins were from cell surface-biotinylated GD25 cells which were cotransfected with a full-length untagged  $\beta$ 1A integrin-pECE and the aforementioned GFP-tagged PKC $\alpha$  V3 domain truncations. All the bound proteins on the protein G bead (Bound) and one-fifth of the unbound proteins left in the cell extract supernatant after the first centrifugation after precipitation (Unbound) were loaded. The blot containing the anti-integrin immunoprecipitates was stripped and re-probed with HRP-conjugated streptavidin (Strep-HRP). Two predominant biotinylated surface proteins were immunoprecipitated using the anti- $\beta$ 1 polyclonal antibody, representing the  $\beta$ 1 integrin  $\alpha/\beta$  heterodimer, as shown in Fig. 5A. Positions of the approximate molecular mass markers are shown. (D) Effects of the same PKC $\alpha$  V3 domain truncation constructs on directional cell motility towards a PDBu gradient, in comparison with GFP vector control-transfected cells (repeat of the experiment in Fig. 1 using different V3 truncation mutants) (see the legend to Fig. 1A).

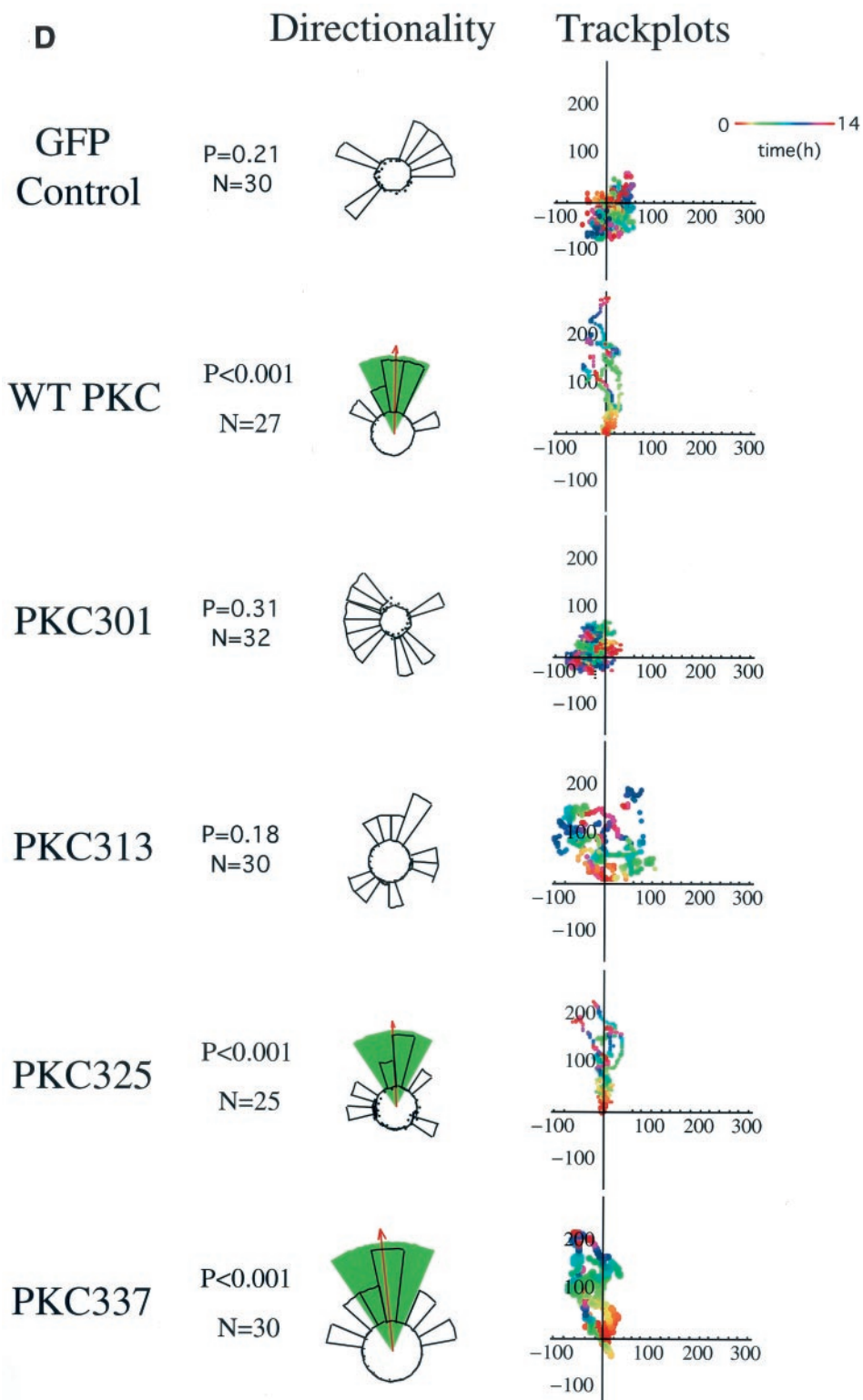


FIG. 6—Continued.

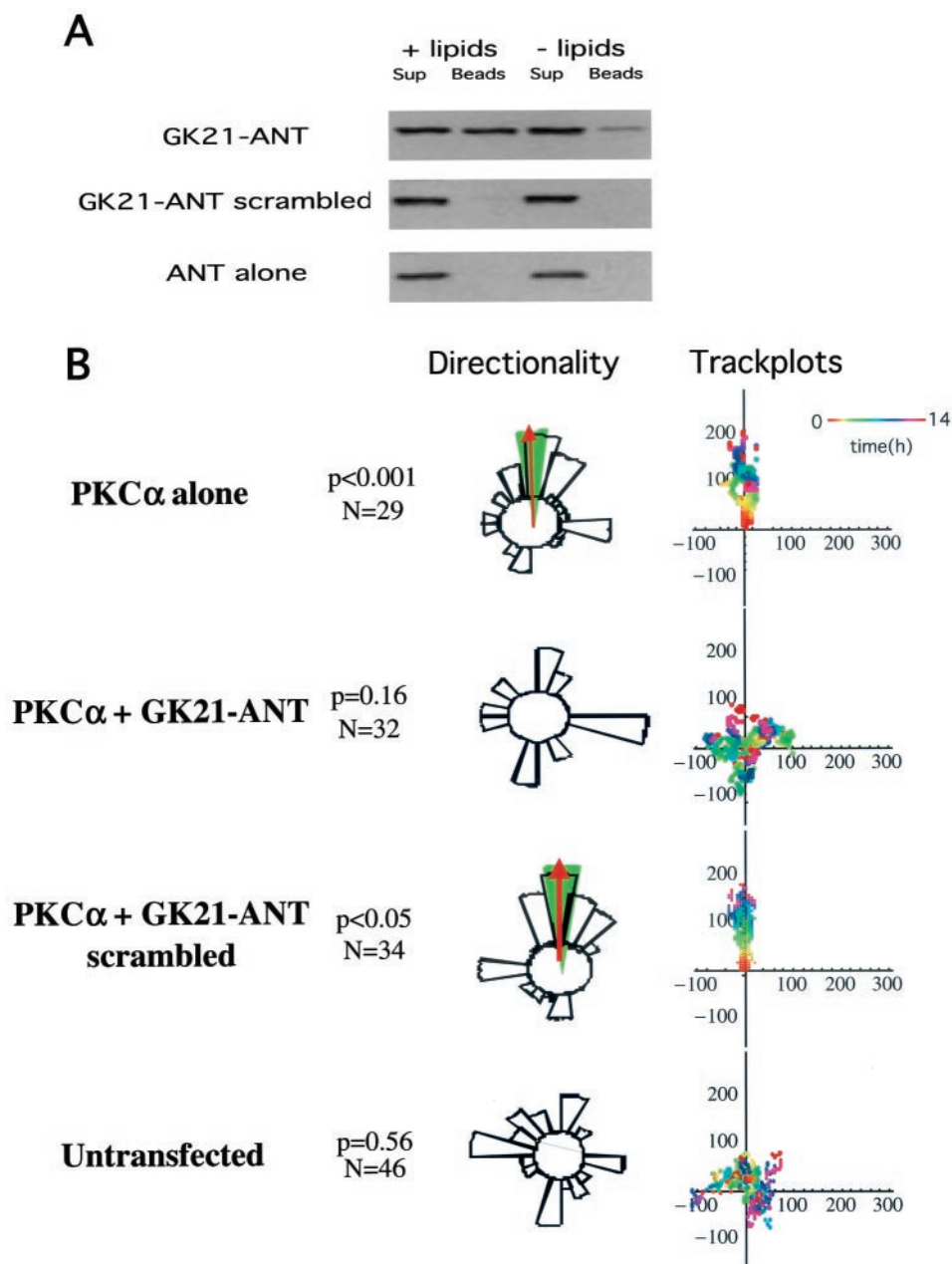


FIG. 7. Effect of a cell-permeant form of GK21 on breast carcinoma cell chemotaxis. (A) In the presence of PS and TPA (+ lipids), full-length GFP-PKC $\alpha$  was bound to the GK21 peptide manufactured by chemical synthesis in tandem with the antennapedia third helix (residues 43 to 58) sequence (GK21-ANT), but not its scrambled version (GK21-ANT scrambled) or the antennapedia sequence alone (ANT). For each sample, all of the peptide-bound GFP-PKC $\alpha$  (Beads) was run alongside one-fifth of the corresponding supernatant containing unbound proteins (Sup). (B) MCF-7 cells transiently expressing the full-length GFP-PKC $\alpha$  exhibited significant directional chemotaxis towards a PDBu gradient in a Dunn chamber ( $P < 0.001$ ). This PKC-driven directional motility was eliminated by pretreating cells with 8  $\mu$ M of a cell-permeant (antennapedia-tagged), rhodaminated form of GK21 (GK21-ANT), but not its scrambled version. See the legend to Fig. 1A for explanation of track plots. (C) Untransfected MDA-MB-231 cells exhibited significant directional chemotaxis towards an EGF gradient in a Dunn chamber (0.1  $\mu$ M in the outer well,  $P < 0.001$ ). Chemotaxis towards EGF was eliminated by pretreating cells with 8  $\mu$ M of a cell-permeant (antennapedia-tagged), rhodaminated form of GK21 (GK21-ANT), but not its scrambled version.

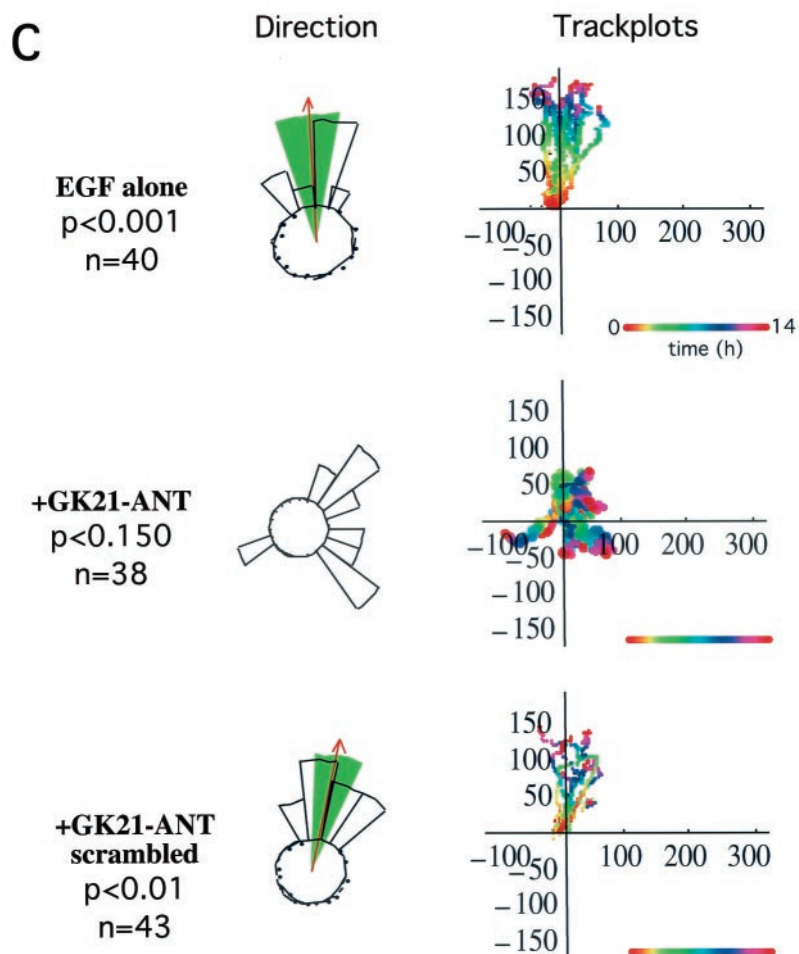


FIG. 7—Continued.

beled anti- $\beta 1$  integrin IgG Fab fragments. These latter data place the fluorophore pair within nanometer proximity (9, 15–17, 19, 30). Recently, PKC $\alpha$  was also shown to coprecipitate with the integrin  $\alpha 3$  and  $\alpha 6$  subunits as well as CD81, a member of the transmembrane 4 superfamily (TM4SF), providing strong evidence for the existence of PKC $\alpha$ -TM4SF- $\alpha 3/\alpha 6$   $\beta 1$  integrin complexes (34). For each of these complexes, there appears to be at least three direct interaction pairs, with the binding sites either fully or partially identified (PKC $\alpha$ - $\beta 1$  integrin [Fig. 2 to 6], TM4SF-PKC $\alpha$  [34], and TM4SF-integrin [3, 13, 31]). The coprecipitation assays show that the  $\beta 1$  integrin Cyto-2 and Cyto-3 amino acid clusters are both involved in integrin/PKC $\alpha$  complex formation. It is notable that the tyrosine residues of the two NPXY motifs have already been shown to be important for directed cell migration through integrin substrate-coated filters in response to growth factor chemotactic gradients (22, 23). Our finding of a dominant inhibitory effect of the Cyto-2- and Cyto-3-containing  $\beta 1$  tail sequence on directional cell migration, when introduced into cells either as a cell-permeant peptide or through retroviral transduction, has not previously been reported, and is consistent with these earlier studies documenting the effects of various NPXY  $\beta 1A$  mutants upon directional cell movement.

The introduction of a Cyto-2- and Cyto-3-containing  $\beta 1$  integrin cytoplasmic sequence, as a cell-permeant peptide, is demonstrated here to eliminate PKC-mediated chemotaxis of breast carcinoma cells. Preincubation of GST-PKC $\alpha$  RD+V3 on glutathione beads with free GK peptide, not its scrambled equivalent, eliminated its ability to associate with  $\beta 1$  integrin in vitro. Besides PKC $\alpha$ , another  $\beta 1$  integrin-binding protein targeted by the GK peptide sequence is integrin cytoplasmic domain-associated protein 1 (ICAP-1) (6). Further work is required to establish the temporal relationship between PKC $\alpha$  and ICAP-1 binding to this distal  $\beta 1$  cytoplasmic region in the context of cell motility.

EGF receptor is expressed aberrantly in approximately 40% of breast carcinomas; signaling through this growth factor receptor is interdependent on that of  $\beta 1$  integrin (28). Both the cell-permeant ANT-GK21 peptide and the retrovirally encoded version of the peptide inhibitor, based on the PKC $\alpha$ -binding sequence of  $\beta 1$  integrin, were shown to be effective against the directed cell movement towards EGF, a pathophysiologically relevant chemoattractant for these breast carcinoma cells.

A constitutive protein complex formed between PKC $\alpha$  and  $\beta 1$  integrin has also been found in multiple myeloma cells (20).

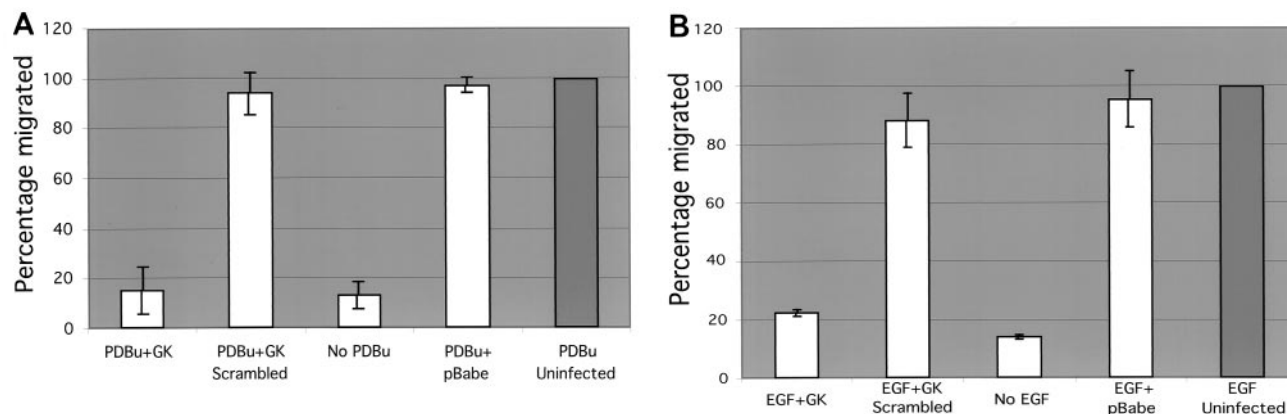


FIG. 8. Retroviral transduction of a minigene insert encoding the GK21 sequence eliminated EGF-induced chemotaxis. MDA-MB231 cells were infected with media from Phoenix packaging cells containing the intact retrovirus encoding the myc epitope-tagged GK21  $\beta$ 1 cytoplasmic sequence, its scrambled equivalent, or the pBabe vector alone. Retroviral transduction efficiency was checked using parallel cultures that were fixed and stained with an anti-myc MAb 9E10. At 48 h postinfection, 231 cells were trypsinized and subjected to an 8-h Transwell chamber migration assay (described in Materials and Methods). Cell harvesting and counting were performed in a blind manner by two individuals, and the subsequent decoding of the samples was carried out by a third investigator. Approximately 10 and 14% of uninfected cells migrated through the filter towards the PDBu (A) and EGF (B) gradients, respectively, over the 8-h time course. The percentage of the cell population that migrated (lower well cell count/upper well cell count) following each treatment was normalized against the mean percentage of uninfected cells that migrated (set at 100%) in the same experiment. Presented are the mean percentages of cells that migrated  $\pm$  standard deviations from  $n = 3$  wells for each treatment. Results are representative of three independent experiments.

When plated on a  $\beta$ 1 integrin substrate, these myeloma cells can be stimulated to migrate in response to vascular endothelial growth factor (VEGF) which induces PKC $\alpha$  (but not PKC $\epsilon$ ) membrane translocation and activation in a phosphoinositide 3-kinase-dependent manner. Furthermore, in these melanoma studies, the use of a  $\beta$ 1 integrin blocking antibody and the PKC inhibitor bisindolylmaleimide clearly illustrated a dominant role for the PKC $\alpha$ - $\beta$ 1 integrin signaling complex in

the development of a VEGF-responsive, migratory phenotype. Importantly, our new findings have clearly defined the molecular determinants underlying the formation of this protein complex as well as the PKC-mediated component of directional cell motility. In addition, the results of the present study using a retrovirally encoded inhibitor provide evidence that interference in the PKC $\alpha$ - $\beta$ 1 integrin interaction will suppress the migratory phenotype associated with metastatic disease.

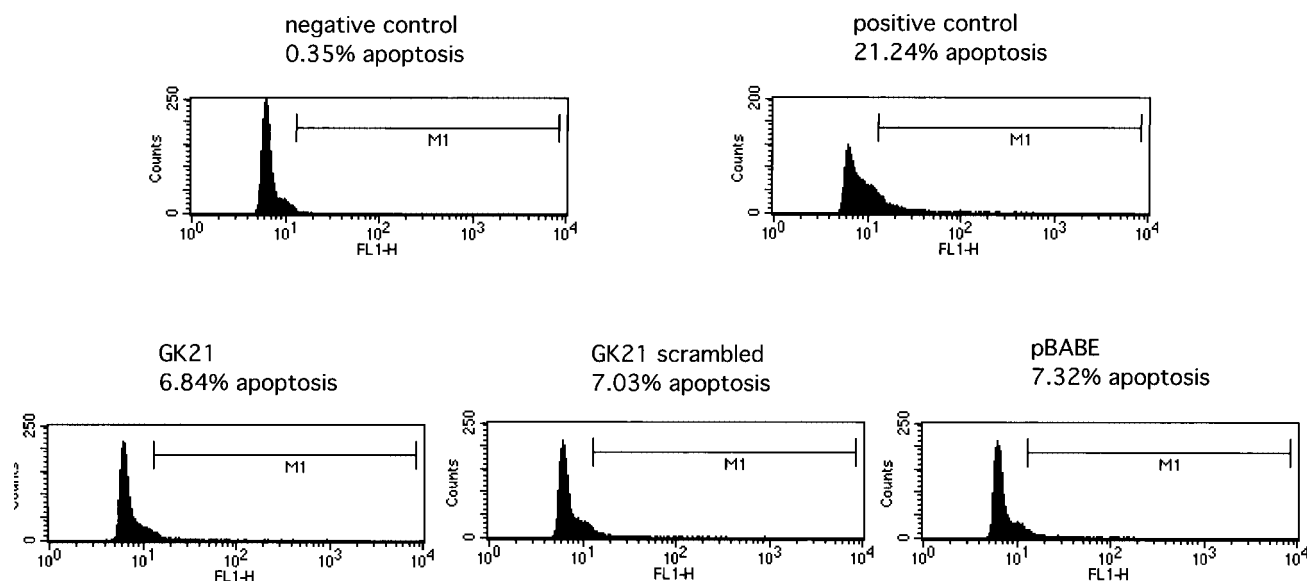


FIG. 9. The effect of introducing retroviral constructs encoding the pBABE vector alone, GK21, or scrambled sequence of GK21 on cell survival was evaluated by a TUNEL assay (Promega). Positive-control cells were incubated with 30  $\mu$ M genistein for 48 h. Apoptosis was monitored by the amount of TdT-mediated fluorescein-conjugated dUTP uptake, as detected by fluorescence-activated cell sorting analysis. M1 denotes the subset of cells displaying a significant degree of apoptosis above the negative cutoff, which was determined by the amount of fluorescein-conjugated dUTP incorporated in the absence of TdT. Results are representative of two independent experiments.

## ACKNOWLEDGMENTS

M. Parsons and M. Keppler contributed equally to this work.

We are particularly indebted to James Monypenny for technical assistance during the time-lapse experiments and image processing. We thank John Marshall and Fiona Watt for reviewing the manuscript and many helpful suggestions. A rabbit polyclonal antiserum against human  $\beta 1$  integrin was kindly provided by J. Ivaska.

This study was supported in part by the Cancer Research United Kingdom, the United Kingdom Medical Research Council (in the form of a Clinician Scientist Grant awarded to T.N.) and the Wellcome Trust (M.J.H.).

## REFERENCES

- Bailly, M., J. Wyckoff, B. Bouzahzah, R. Hammerman, V. Sylvestre, M. Cammer, R. Pestell, and J. E. Segall. 2000. Epidermal growth factor receptor distribution during chemotactic responses. *Mol. Biol. Cell* **11**:3873–3883.
- Bastiaens, P. I. H., and T. M. Jovin. 1998. Fluorescence resonance energy transfer microscopy, p. 136–146. *In* J. Celis (ed.), *Cell biology: a laboratory handbook*. Academic Press, New York, N.Y.
- Berditchevski, F., G. Bazzoni, and M. E. Hemler. 1995. Specific association of CD63 with the VLA-3 and VLA-6 integrins. *J. Biol. Chem.* **270**:17784–17790.
- Berrier, A. L., A. M. Mastrangelo, J. Downward, M. Ginsberg, and S. E. LaFlamme. 2000. Activated R-Ras, Rac1, PI 3-kinase and PKC $\epsilon$  can each restore cell spreading inhibited by isolated integrin  $\beta 1$  cytoplasmic domains. *J. Cell Biol.* **151**:1549–1560.
- Bretscher, M. S. 1996. Moving membrane up to the front of migrating cells. *Cell* **85**:465–467.
- Chang, D. D., C. Wong, H. Smith, and J. Liu. 1997. ICAP-1, a novel  $\beta 1$  integrin cytoplasmic domain-associated protein, binds to a conserved and functionally important NPXY sequence motif of  $\beta 1$  integrin. *J. Cell Biol.* **138**:1149–1157.
- Dufour, S., J. L. Duband, M. J. Humphries, M. Obara, K. M. Yamada, and J. P. Thiery. 1988. Attachment, spreading and locomotion of avian neural crest cells are mediated by multiple adhesion sites on fibronectin molecules. *EMBO J.* **7**:2661–2671.
- Ellis, L., E. Clauser, D. O. Morgan, M. Ederly, R. A. Roth, and W. J. Rutter. 1986. Replacement of insulin receptor tyrosine residues 1162 and 1163 compromises insulin-stimulated kinase activity and uptake of 2-deoxyglucose. *Cell* **45**:721–732.
- Herreros, J., T. Ng, and G. Schiavo. 2001. Lipid rafts act as specialized domains for tetanus toxin binding and internalization into neurons. *Mol. Biol. Cell* **12**:2947–2960.
- LaFlamme, S. E., L. A. Thomas, S. S. Yamada, and K. M. Yamada. 1994. Single subunit chimeric integrins as mimics and inhibitors of endogenous integrin functions in receptor localization, cell spreading and migration, and matrix assembly. *J. Cell Biol.* **126**:1287–1298.
- Lawson, M. A., and F. R. Maxfield. 1995. Ca<sup>2+</sup>- and calcineurin-dependent recycling of an integrin to the front of the migrating neutrophils. *Nature* **377**:75–79.
- Maaser, K., K. Wolf, C. E. Klein, B. Niggemann, K. S. Zanker, E. B. Brocker, and P. Friedl. 1999. Functional hierarchy of simultaneously expressed adhesion receptors: integrin  $\alpha 2\beta 1$  but not CD44 mediates MV3 melanoma cell migration and matrix reorganization within three-dimensional hyaluronan-containing collagen matrices. *Mol. Biol. Cell* **10**:3067–3079.
- Mannion, B. A., F. Berditchevski, S. K. Kraeft, L. B. Chen, and M. E. Hemler. 1996. Transmembrane-4 superfamily proteins CD81 (TAPA-1), CD82, CD63, and CD53 specifically associated with integrin  $\alpha 4\beta 1$  (CD49d/CD29). *J. Immunol.* **157**:2039–2047.
- Mastrangelo, A. M., S. M. Homan, M. J. Humphries, and S. E. LaFlamme. 1999. Amino acid motifs required for isolated  $\beta$  cytoplasmic domains to regulate “in trans”  $\beta 1$  integrin conformation and function in cell attachment. *J. Cell Sci.* **112**:217–229.
- Ng, T., M. Parsons, W. E. Hughes, J. Monypenny, D. Zicha, A. Gautreau, M. Arpin, S. Gschmeissner, P. J. Verveer, P. I. Bastiaens, and P. J. Parker. 2001. Ezrin is a downstream effector of trafficking PKC-integrin complexes involved in the control of cell motility. *EMBO J.* **20**:2723–2741.
- Ng, T., D. Shima, A. Squire, P. I. H. Bastiaens, S. Gschmeissner, M. J. Humphries, and P. J. Parker. 1999. PKC $\alpha$  regulates  $\beta 1$  integrin-dependent motility, through association and control of integrin traffic. *EMBO J.* **18**:3909–3923.
- Ng, T., A. Squire, G. Hansra, F. Bornancin, C. Prevostel, A. Hanby, W. Harris, D. Barnes, S. Schmidt, H. Mellor, P. I. H. Bastiaens, and P. J. Parker. 1999. Imaging PKC  $\alpha$  activation in cells. *Science* **283**:2085–2089.
- Oancea, E., and T. Meyer. 1998. Protein kinase C as a molecular machine for decoding calcium and diacylglycerol signals. *Cell* **95**:307–318.
- Parsons, M., and T. Ng. 2002. Intracellular coupling of adhesion receptors: molecular proximity measurements. *Methods Cell Biol.* **69**:261–278.
- Podar, K., Y. T. Tai, B. K. Lin, R. P. Narsimhan, M. Sattler, T. Kijima, R. Salgia, D. Gupta, D. Chauhan, and K. C. Anderson. 2001. Vascular endothelial growth factor (VEGF)-induced migration of multiple myeloma cells is associated with  $\beta 1$ -integrin- and PI3-kinase-dependent PKC $\alpha$  activation. *J. Biol. Chem.* **20**:20.
- Rigot, V., M. Lehmann, F. Andre, N. Daemi, J. Marvaldi, and J. Luis. 1998. Integrin ligation and PKC activation are required for migration of colon carcinoma cells. *J. Cell Sci.* **111**:3119–3127.
- Sakai, T., O. Peyruchaud, R. Fassler, and D. F. Mosher. 1998. Restoration of  $\beta 1$  A integrins is required for lysophosphatidic acid-induced migration of  $\beta 1$ -null mouse fibroblastic cells. *J. Biol. Chem.* **1998**:19378–19382.
- Sakai, T., Q. Zhang, R. Fassler, and D. F. Mosher. 1998. Modulation of  $\beta 1$  A integrin functions by tyrosine residues in the  $\beta 1$  cytoplasmic domain. *J. Cell Biol.* **141**:527–538.
- Squire, A., and P. I. H. Bastiaens. 1999. Three dimensional image restoration in fluorescence lifetime imaging microscopy. *J. Microsc.* **193**:36–49.
- Taunton, J. 2001. Actin filament nucleation by endosomes, lysosomes and secretory vesicles. *Curr. Opin. Cell Biol.* **13**:85–91.
- Taunton, J., B. A. Rowning, M. L. Coughlin, M. Wu, R. T. Moon, T. J. Mitchison, and C. A. Larabell. 2000. Actin-dependent propulsion of endosomes and lysosomes by recruitment of N-WASP. *J. Cell Biol.* **148**:519–530.
- Vallentin, A., C. Prevostel, T. Fauquier, X. Bonnefont, and D. Joubert. 2000. Membrane targeting and cytoplasmic sequestration in the spatiotemporal localization of human protein kinase C  $\alpha$ . *J. Biol. Chem.* **275**:6014–6021.
- Wang, F., V. M. Weaver, O. W. Petersen, C. A. Larabell, S. Dedhar, P. Briand, R. Lupu, and M. J. Bissell. 1998. Reciprocal interactions between  $\beta 1$ -integrin and epidermal growth factor receptor in three-dimensional basement membrane breast cultures: a different perspective in epithelial biology. *Proc. Natl. Acad. Sci. USA* **95**:14821–14826.
- Weaver, V. M., O. W. Petersen, F. Wang, C. A. Larabell, P. Briand, C. Damsky, and M. J. Bissell. 1997. Reversion of the malignant phenotype of human breast cells in three-dimensional culture and in vivo by integrin blocking antibodies. *J. Cell Biol.* **137**:231–245.
- Wouters, F. S., P. J. Verveer, and P. I. Bastiaens. 2001. Imaging biochemistry inside cells. *Trends Cell Biol.* **11**:203–211.
- Yauch, R. L., F. Berditchevski, M. B. Harler, J. Reichner, and M. E. Hemler. 1998. Highly stoichiometric, stable, and specific association of integrin  $\alpha 3\beta 1$  with CD151 provides a major link to phosphatidylinositol 4-kinase, and may regulate cell migration. *Mol. Biol. Cell* **9**:2751–2765.
- Yehra, M., E. J. Filardo, E. M. Bayna, E. Kawahara, J. C. Becker, and D. A. Cheresh. 1995. Induction of carcinoma cell migration on vitronectin by NF- $\kappa$ B-dependent gene expression. *Mol. Biol. Cell* **6**:841–850.
- Young, S., J. Rothbard, and P. J. Parker. 1988. A monoclonal antibody recognising the site of limited proteolysis of protein kinase C. Inhibition of down-regulation in vivo. *Eur. J. Biochem.* **173**:247–252.
- Zhang, X. A., A. L. Bontrager, and M. E. Hemler. 2001. Transmembrane-4 superfamily proteins associate with activated protein kinase C (PKC) and link PKC to specific  $\beta 1$  integrins. *J. Biol. Chem.* **276**:25005–25013.
- Zicha, D., W. E. Allen, P. M. Brickell, C. Kinnon, G. A. Dunn, G. E. Jones, and A. J. Thrasher. 1998. Chemotaxis of macrophages is abolished in the Wiskott-Aldrich syndrome. *Br. J. Haematol.* **101**:659–665.
- Zicha, D., G. Dunn, and G. Jones. 1997. Analyzing chemotaxis using the Dunn direct-viewing chamber, p. 449–457. *In* J. W. Pollard and J. M. Walker (ed.), *Basic cell culture protocols*, 2nd ed., vol. 75. Humana Press Inc., Totowa, N.J.